ELSEVIER

Cement and Concrete Composites **20** (1998) 419–435

0958-9465/98/$ — see front matter

PII:S0958-9465(98)00028-6

Unified Approach to Shear Analysis and Design

Thomas T. C. Hsu

University of Houston, Houston, TX 77204, USA

Abstract

The theory of reinforced concrete originated in the late 19th century with the development of the linear theory for bending. As the first rational theory in reinforced concrete behavior, it satisfied Navier's three principles of mechanics of materials: stress equilibrium; strain compatibility; and constitutive law of material. By the 1950s this linear bending theory was generalized to become the Bernoulli compatibility truss model which covered both the linear and non-linear theories for bending, axial load and their combination. For shear and torsion, however, a rational theory that satisfies Navier's principles took the entire 20th century to develop. By the 1990s the theory for shear and torsion contained four truss models: the equilibrium (plasticity) truss model; the Mohr compatibility truss model; the rotating-angle softened-truss model; and the fixed-angle softened-truss model. Together with the strut-and-tie model for local regions and the Bernoulli compatibility truss model for bending and axial load, a unified theory of six rational models for reinforced concrete was established.The two nonlinear softened-truss models have capacities for predicting the behavior of reinforced concrete elements subjected to in-plane shear and normal stresses. These two models satisfy the two-dimensional stress equilibrium, Mohr's circular strain compatibility and the softened biaxial constitutive laws of concrete. As a result, they can be used to predict the strength as well as the load-deformation history of a membrane element. The rotating-angle softened-truss model is simple to use and is adequate for situation that does not require the 'contribution of concrete' (V_c), while the fixed-angle softened-truss model is more complex but is capable of predicting V_c.The rotating-angle softened-truss model has been used to analyze four types of structures that are subjected predominantly to shear: low-rise shear walls, framed shear walls, deep beams and shear transfer zones. In addition, both softened truss models are used to construct the concrete stiffness matrices used in the finite element analysis. These matrices contain only three moduli in the diagonal elements. The assumption that Poisson ratios are zero in the non-diagonal elements leads to undesirable limitations of applicability. To overcome this weakness, a general model of the stiffness matrix is proposed that includes two additional Poisson ratios. All five material properties in the general matrix are currently being established by new biaxial tests of panels using proportional loading and strain-control procedures. © 1998 Elsevier Science Ltd. All rights reserved.

Keywords: design, plasticity, reinforced concrete, shear, strut-and-tie model, truss model.

NOTATION

a	Shear span of beams
b	Width of beam cross sections or thickness of walls and panels
B	A parameter defined as $(1/\rho)(f_{cr}/f_y)^{1.5}$
d	Effective depth of cross section or walls
d_v	Distance between the centroids of the top and bottom stringers
d_w	Effective horizontal length of wall, measured between centroids of boundary elements
E_c	Modulus of elasticity of concrete, taken as 3875 $\sqrt{f'_c}$ (f'_c and $\sqrt{f'_c}$ are in MPa) for tension
E_s	Modulus of elasticity of bare steel bars

$\bar{E}_d, \bar{E}_r$ Secant moduli of concrete in the principal d- and r-direction, respectively

$\bar{E}_2, \bar{E}_1$ Secant moduli of concrete in the principal 2- and 1-direction, respectively

f_ℓ, f_t Average steel stresses in longitudinal (ℓ-) and transverse (t-) directions, respectively

f_n Average stress of mild steel bars embedded in concrete at the beginning of yielding, defined at the intersection of the two straight lines in the bilinear model

f_s Average stress in mild steel bars. f_s becomes f_ℓ or f_t when applied to longitudinal steel or transverse steel, respectively

f_y Yield stress of bare mild steel bars, representing the local yield stress of 90° reinforcing bars at cracks. f_y becomes $f_{\ell y}$ or f_{ty} when applied to longitudinal steel or transverse steel, respectively

f_{cr} Cracking stress of concrete, taken as $0{\cdot}31\sqrt{f_c'}$ (f_c' and $\sqrt{f_c'}$ are in MPa)

f_c' Maximum compressive strength of standard 6 in × 12 in concrete cylinder

f_y' Average yield stress of mild steel bars embedded in concrete. It is not a constant, but is a linear function of the average steel strain ε_s. f_y' becomes $f_{\ell y}'$ or f_{ty}', when applied to longitudinal steel or transverse steel, respectively

$\bar{G}_{dr}$ Secant shear modulus of concrete with respect to the principal d–r coordinate

$\bar{G}_{21}$ Secant shear modulus of concrete with respect to the principal 2–1 coordinate

h Total depth of beams or width of panel in shear transfer test specimens

h_w Height of wall

K A coefficient or constant relating the stresses $\tau_{\ell t}$ and σ_t in deep beams or shear transfer test specimens

K_σ, K_τ Coefficients describing the non-uniform distribution of stresses in shear transfer test specimens

l Total length of shear plane in shear transfer test specimens

P_t A pair of forces acting along the shear plane of shear transfer test specimens

v_u Ultimate shear stress

V Shear force

V_n Nominal shear force in shear walls

α Rotating-angle; angle between the principal compressive stress of concrete (d-axis) and the longitudinal steel bars (ℓ-axis)

α_2 Fixed-angle or steel bar angle; angle between the applied principal compressive stress (2-axis) and the longitudinal steel bars (ℓ-axis)

γ_{dr} Average shear strain in principal d–r coordinate of cracked concrete

$\gamma_{\ell t}$ Average shear strain in ℓ–t coordinate of reinforcing bars (positive as shown in Fig. 1 for $\tau_{\ell t}$)

γ_{21} Average shear strain in principal 2–1 coordinate of applied stresses

γ_{21m} Average shear strain corresponding to τ_{21m}^c

$\varepsilon_d, \varepsilon_r$ Average strains in principal d- and r-directions of cracked concrete, respectively, (positive for tension)

$\varepsilon_\ell, \varepsilon_t$ Average strains in ℓ- and t-directions of reinforcing bars, respectively, (positive for tension)

ε_n Average yield strain of mild steel bars embedded in concrete at the beginning of yielding. $\varepsilon_n = \varepsilon_y(0{\cdot}93 - 2B)$

ε_s Average strain in the mild steel bars embedded in concrete. ε_s becomes ε_ℓ or ε_t, when applied to longitudinal and transverse steel, respectively

ε_y Yield strain in bare mild steel bars. $\varepsilon_y = f_y/E_s$

ε_{cr} Tensile cracking strain of concrete, taken as 0·00008

ε_o Concrete strain at maximum compressive strength, taken as 0·002

$\varepsilon_2, \varepsilon_1$ Average strains in principal 2- and 1-directions of applied stresses, respectively (positive for tension)

ζ Softened coefficient of concrete in compressive stress–strain curve

η A parameter defined as $(\rho_t f_{ty} - \sigma_t)/(\rho_\ell f_{\ell y} - \sigma_\ell)$, becomes $\rho_t f_{ty}/\rho_\ell f_{\ell y}$ when $\sigma_t = \sigma_\ell = 0$

η' A parameter defined as η or $1/\eta$ whichever is less than unity

ν Poisson ratio

ν_{12} Tension–compression Poisson ratio of cracked concrete in the 2–1 coordinate

ν_{21} Compression–tension Poisson ratio of cracked concrete in the 2–1 coordinate

ξ Pre-yield reinforcement index defined as $f_{\ell y}/E_s\varepsilon_0$

ρ Steel reinforcement ratio. ρ becomes ρ_ℓ or ρ_t, when applied to longitudinal steel or transverse steel, respectively

ρ_ℓ, ρ_t Steel reinforcement ratios in the longitudinal (ℓ-) and transverse (t-) directions, respectively

σ_d, σ_r Average concrete stresses in principal d- and r-directions, respectively (positive for tension)

σ_ℓ, σ_t Applied normal stresses in ℓ- and t-directions of reinforcing bars, respectively (positive for tension)

σ_2, σ_1 Applied principal stresses in the 2- and 1-directions, respectively

σ_2^c, σ_1^c Average normal stresses of concrete in principal 2- and 1-directions of applied stresses, respectively

τ_{dr} Average shear stress in principal d–r coordinate of cracked concrete

$\tau_{\ell t}$ Applied shear stress in ℓ–t coordinate of reinforcing bars (positive as shown in Fig. 1)

τ_n Nominal shear stress in shear walls

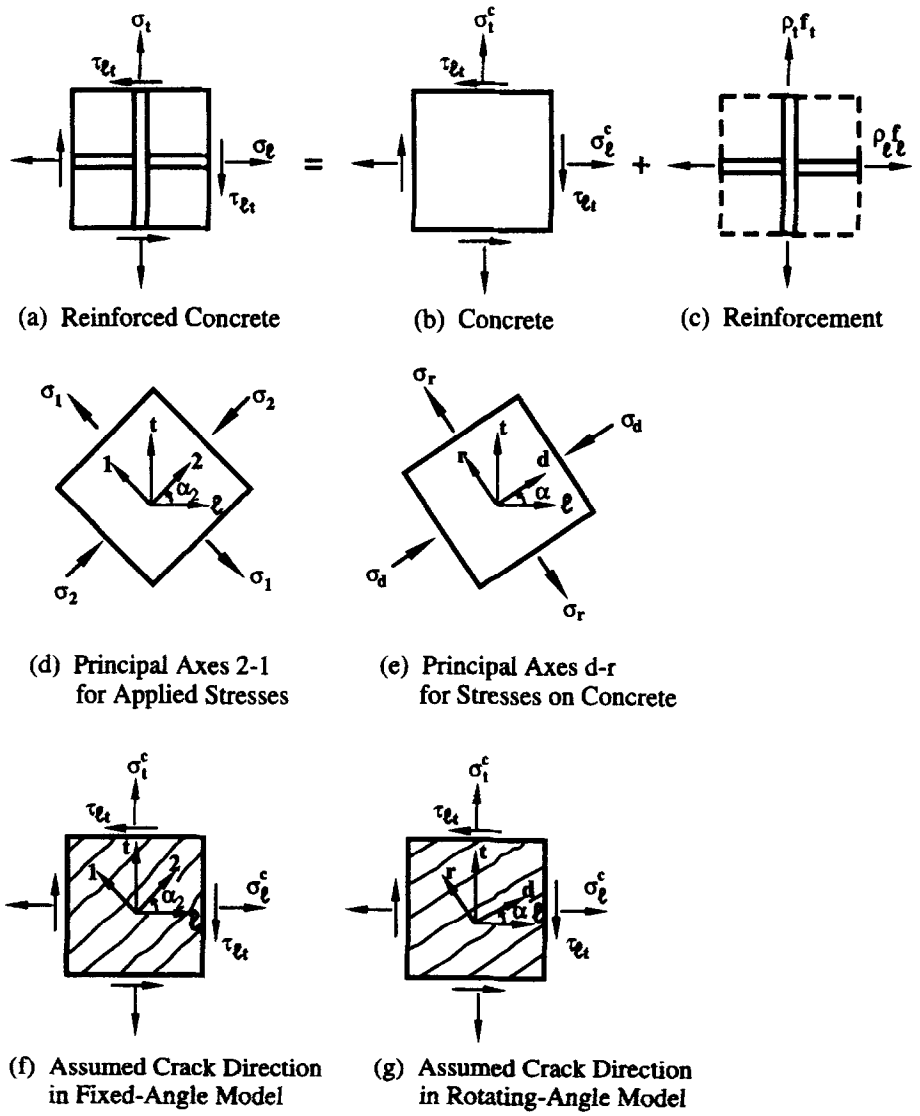

Fig. 1. Reinforced concrete membrane elements subjected to in-plane stresses. (a) Reinforced concrete, (b) concrete, (c) reinforcement, (d) principal axes 2–1 for applied stresses, (e) principal axes d–r for stresses on concrete, (f) assumed crack direction in fixed-angle model and (g) assumed crack direction in rotating-angle model.

τ_{nb} Balanced nominal shear stress in shear walls

τ^c_{21} Average shear stress of concrete in principal 2–1 coordinate of applied stresses

τ^c_{21m} Average shear stress of concrete in the principal 2–1 coordinate at maximum applied stress

ω Reinforcement index defined as $\rho f_y/f'_c$. ω becomes $\omega_l = \rho_l f_{ly}/f'_c$ and $\omega_t = \rho_t f_{ty}/f'_c$ when applied to longitudinal and transverse directions, respectively

BACKGROUND: PRINCIPLES OF MECHANICS OF MATERIALS

Homogeneous and linear materials

The behavior of a beam subjected to bending was first investigated by Galileo in 1638. In his famous book "Dialogues on Two New Sciences", he studied the equilibrium of a stone cantilever beam of rectangular section and found that the beam could support twice as much load at the center as at the free end, because the same moment was produced at the fixed end. Using such rudimentary knowledge of statics, he observed that for beams "of equal length but unequal thickness, the resistance to fracture increases in the same ratio as the cube of the thickness", provided that the shape (i.e. thickness/width ratio) remained unchanged. Since his beams were considered rigid bodies, beam deflections could not be evaluated, thus creating the mystery known as 'Galileo's problem'.

The solution to Galileo's problem required the principle of equilibrium and two additional sources of information. The first source came from an understanding of the mechanical properties of material summarized as follows. In 1678, Hooke observed that for specimens of various materials under light load, the deformation is proportional to the force. In 1705, James Bernoulli, one member of a family of Swiss scholars, defined the concept of stress (force divided by area) and strain (displacement divided by original length). This was followed by Euler's postulation in 1727 of Hooke's law for elastic materials, that is, stress and strain increase proportionally. The proportionality constant was defined in 1804 as Young's modulus, E.

The second source of information came from the observation of deformations in beams. In relating the radius of curvature of a beam to the bending moment, Jacob Bernoulli, James' brother, postulated in 1705 the well-known 'Bernoulli's hypothesis', that is, 'plane section remains plane'. It should be noted that Jacob Bernoulli misunderstood the neutral axis and took it at the concave surface of the beam. As a result, his derived flexural rigidity (EI) was twice the correct value. Nevertheless, based on Bernoulli's hypothesis and assuming the proportionality between curvature and bending, Euler derived in 1757 the elastic deflection curve of a beam by using the then newly developed mathematical tool of calculus. However, Euler was unable to theoretically derive the flexural rigidity, EI.

As history bears out, the correct derivation of the flexural rigidity EI, the key to the solution of Galileo's problem, requires the integration of all three sources of information on stress equilibrium, strain compatibility and Hooke's law of material. These three principles were first put together in a correct way by a French engineer, Coulomb, in 1773. Later in 1826 a French professor, Navier, presented a landmark book[1] in which he systematically and rigorously derived the bending theory using these three principles. Navier's comprehensive book included most of the topics covered in modern textbooks on the mechanics of materials, including the solutions for flexure, axial loads, shear, and torsion (circular sections only). It also showed that a correct load-deformation relationship of a beam must be analyzed according to the three principles of the mechanics of materials. He showed that these principles were applicable not only to bending and axial load, but also to shear and torsion.

Reinforced concrete

Reinforced concrete came into being four decades after Navier's book. Its birth was credited to Joseph Monier, a French gardener, who obtained a patent in 1867 for reinforcing the concrete in his flower pots with iron wires. The concept of using metal reinforcement to overcome the weakness of concrete in tension was quickly adapted to buildings and bridges, and the use of reinforced concrete for construction became widely accepted in the last quarter of the 19th century. Such growth in applications

gave rise to the demand for a rational theory to analyze and design reinforced concrete. By the end of the 19th century a linear bending theory for cracked reinforced concrete began to emerge. Not surprisingly, this theory was developed by French engineers (e.g. Coignet, Hennibique) who employed the three principles of mechanics of materials as in Navier's book. Because Hooke's linear stress–strain relationships were employed, we have the linear bending theory that is applicable up to the service load stage. This theory served as the basis of the allowable stress design method which was used in the ACI Code from its inception in 1910 until 1963.

In the 1950s, the non-linear constitutive laws of concrete and steel were used in conjunction with the parallel stress equilibrium and Bernoulli's linear compatibility to solve the bending problem. This non-linear bending theory could be used to accurately predict the behavior of a beam up to failure and served as the basis for the ultimate strength design method which was introduced into the 1963 ACI Code. Although the non-linear stress–strain relationship of concrete should have followed Hognestad *et al.* stress–strain curve determined from the dog-bone specimens[2], the ACI Code allowed Hognestad's compression stress block to be replaced by Whitney's equivalent rectangular stress block at the ultimate load stage[3].

Both the linear and non-linear theories for bending can be expanded to analyze and design members subjected to combined bending and axial loads. These theories for bending and axial load are now known collectively as the Bernoulli compatibility truss model. The inclusion of this rational model in the 1963 ACI code was a milestone that signified its general acceptance. This model is rational because it is founded on Navier's three principles of the mechanics of materials.

In contrast, a rational theory for shear and torsion has had a much more complex developmental history, spanning the entire 20th century. This paper will first describe the basic concepts supporting a unified theory for shear in reinforced concrete. It will then show how the equations for stress equilibrium, strain compatibility and constitutive laws of concrete and steel were developed for the four shear models; and lastly, it will describe the applications of the two non-linear shear models.

BASIC CONCEPTS IN SHEAR MODELS

Model with linear elements versus model with membrane elements

The use of a truss concept to simulate the action of a reinforced concrete beam subjected to shear and bending originated at the turn of the century by Ritter[4] and Mörsch[5]. They viewed a reinforced concrete member as an assembly of two types of linear elements: the compressive concrete struts and the tensile steel ties. Although the struts and ties are idealized as lines without cross sectional dimensions, the forces in these linear elements are obliged to satisfy the equilibrium condition at the joints (points of intersection). This model with linear elements was frequently found to overestimate the shear and torsional strengths of reinforced concrete members.

By the 1960s, however, a new concept was applied to reinforced concrete members subjected to shear or torsion. A member was conceived as an assembly of continuous two-dimensional elements, where Navier's three principles of mechanics of materials can be applied. This model with membrane elements gave rise to three rational truss models with increasing sophistication. The application of Navier's first principle of two-dimensional equilibrium resulted in the "equilibrium (plasticity) truss model"[6,7]. The application of the second principle of two-dimensional compatibility gave rise to the "Mohr compatibility truss model"[8–10]; and the application of the third principle of two-dimensional materials laws provided impetus to the development of the "softened truss models"[11–14]. These three models with membrane elements are still called 'truss models' because Poisson's ratios of concrete are assumed to be zero. Physically, this assumption means that the concrete struts are allowed to receive principal compressive strains without causing an expansion in the perpendicular direction of principal tension, and the steel ties are allowed to elongate in the principal tension direction without causing any lateral strains in the principal compression direction. In short, the two-dimensional strain effect is neglected in the constitutive law of cracked concrete.

Although these 'models with membrane elements' gradually replaced the 'models with linear elements' in the main regions of a mem-

ber where the angle of the concrete struts are regular, the linear elements model remains an effective tool for analyzing the local regions where the angle of the concrete struts are irregular. Such a model, which is based on discrete linear elements with irregular angles, is known as the strut-and-tie model.

Strut-and-tie model for local regions

The 1980s saw the renewed interest and widespread development of the strut-and-tie model[15]. This model is particularly suitable for the analysis of local regions where the stresses and strains are so disturbed and irregular that they are not amenable to mathematical solution. Local regions include the connections between a beam and a column, the ends of a column or a beam, the corbels, the region adjacent to a concentrated load, etc. Much research was carried out to study the 'geometrical discontinuity' where sudden changes in geometry occur; or to study the 'statical discontinuities' where areas are subjected to concentrated loads, support reactions, or prestressed forces. As a result, the strut-and-tie model was considerably refined. Improvements included a better understanding of stress flows, the behavior of various types of 'nodes' where the struts and ties intersect, the recommendations of effective concrete stresses for different types of nodes, and the dimensioning of the cross sectional areas for struts and ties.

The local region itself has been visualized as a free-form truss composed of compression struts and tension ties. The struts and ties are arranged so that the internal forces are in equilibrium with the boundary forces. In this design method the compatibility condition is not satisfied, and the serviceability criteria may not be assured. By understanding the stress flows, the bond between the concrete and the reinforcing bars, and the steel anchorage requirement in a local region we can work to improve serviceability and to prevent undesirable premature failures. A good design for a local region depends, to a large degree, on the experience of the engineer.

Truss models for main regions

Truss models are applicable to the main regions where the stresses and strains are distributed so regularly that they can be easily expressed mathematically. That is, the stresses and strains in the main regions are governed by simple equilibrium and compatibility conditions. To implement the concept of continuous material in membrane elements, the truss models must be based on the smeared crack concept. In this context, the constitutive laws of cracked reinforced concrete must be derived from the average (or smeared) stresses and the average (or smeared) strains. An average stress means an average value of the stresses from a crack to midway between two cracks; an average strain is measured from the displacement over a length that traverses several cracks, thus includes the gaps that constitute the crack widths. The average stress–strain relationships of concrete and steel bars must be established directly from the tests of reinforced concrete panels.

When a reinforced concrete element (panel) is subjected to a set of in-plane stresses that increase proportionally, Fig. 1(a), a succession of cracks develops in increasingly divergent directions in the concrete, Fig. 1(b). The direction of the first crack is determined by the direction of the principal tensile stresses that existed before cracking [2–1 coordinate in Fig. 1(d) and (f)]. The angle between the 2-axis and the ℓ-axis is called the fixed-angle α_2 because it remains constant under proportional loading. After initial cracking, the change in the direction of the subsequent cracks are due to changes in the direction of the principal tensile stresses in the concrete, which, in turn, are dependent on the relative amount of steel in the longitudinal and transverse directions, Fig. 1(c). The direction of the principal tensile stress at any stage of cracking is represented by the d–r coordinate in Fig. 1(e and g). The angle between the d-axis and the ℓ-axis is called the rotating-angle α, because this angle continues to 'rotate' away from the fixed-angle α_2 with increasing proportional loading. Theoretical models may be based either on the rotating-angle or on the fixed-angle.

THE FOUR TRUSS MODELS FOR SHEAR

Equilibrium (plasticity) truss model

The two-dimensional equilibrium condition of reinforced concrete membrane elements subjected to shear and normal stresses was first obtained by Nielsen[16] and Lampert and Thurli-

mann[7]. In their original equations the tensile stress of concrete was neglected ($\sigma_r = 0$). Nowadays, the more general equations which include the stress σ_r are derived using the concept of stress transformation in the membrane element[13]. By referring to the definitions of coordinates in Fig. 1, one can derive the following three equilibrium equations based on the rotating angle α:

Equilibrium equations

$$\sigma_l = \sigma_d \cos^2 \alpha + \sigma_r \sin^2 \alpha + \rho_l f_l \quad (1)$$

$$\sigma_t = \sigma_d \sin^2 \alpha + \sigma_r \cos^2 \alpha + \rho_t f_t \quad (2)$$

$$\tau_{lt} = (-\sigma_d + \sigma_r)\sin \alpha \cos \alpha \quad (3)$$

where the definitions of symbols are given in the list of notation.

At failure, the stresses in the longitudinal and transverse steel are assumed to reach yielding level ($f_l = f_{ly}$ and $f_t = f_{ty}$) at the cracks, while the tensile stress of concrete is neglected ($\sigma_r = 0$). Then eqns (1)–(3) are simplified to yield the following formulas in the case of pure shear without normal stresses ($\sigma_l = \sigma_t = 0$):

$$\tan \alpha = \sqrt{\frac{\rho_t f_{ty}}{\rho_l f_{ly}}} \quad (4)$$

$$\tau_{lt} = \sqrt{\rho_l f_{ly} \rho_t f_{ty}} \quad (5)$$

Equation (5) states that the shear stress at yielding is the geometric mean (square-root-of-the-product average) of the smeared yield stresses, $\rho_l f_{ly}$ and $\rho_t f_{ty}$, of the longitudinal and the transverse steel; while eqn (4) states that the angle of the concrete struts at yielding is the square root of the quotient of these two smeared yield stresses. These two equations are applicable only to the ultimate load stage.

Elfgren[16] was able to use this model to elucidate the interacting relationships among bending, shear and torsion. The work of Nielson, Thurlimann and Elfgren served as the basis for the shear and torsion provisions in the 1978 and 1990 CEB-FIP model codes[17,18], as well as the 1995 ACI Code[19,20].

Mohr compatibility truss model

The two-dimensional compatibility condition can now be derived for the reinforced concrete membrane elements subjected to shear and normal stresses as shown in Fig. 1. Using the principle of transformation of strains, the three compatibility equations can be obtained on the basis of the rotating-angle α as follows[13]

Compatibility equations

$$\varepsilon_l = \varepsilon_d \cos^2 \alpha + \varepsilon_r \sin^2 \alpha \quad (6)$$

$$\varepsilon_t = \varepsilon_d \sin^2 \alpha + \varepsilon_r \cos^2 \alpha \quad (7)$$

$$\gamma_{lt} = 2(-\varepsilon_d + \varepsilon_r)\sin \alpha \cos \alpha \quad (8)$$

From eqns (6) and (7) the crack angle α can be derived:

$$\tan \alpha = \sqrt{\frac{\varepsilon_l - \varepsilon_d}{\varepsilon_t - \varepsilon_d}} \quad (9)$$

The rotating angle α in eqn (9) is determined by the strain compatibility condition at each load stage. It will rotate under increasing proportional loading until reaching the condition of eqn (4), when steel yielding occurs in both directions. Equation (9) was first derived by Collins based on the energy method[9].

The solution of the six equilibrium and compatibility equations, eqns (1)–(3) and eqns (6)–(8), requires four stress–strain relationships for materials: two for concrete and two for steel. For concrete, one relationship is σ_d versus ε_d in the d-direction (principal compression direction), and the other relationship is σ_r versus ε_r in the r-direction (principal tension direction). In the case of mild steel, the two relationships are f_l versus ε_l in longitudinal steel and f_t versus ε_t in transverse steel.

Following the assumptions used in the linear bending theory, the tensile strength of concrete is neglected ($\sigma_r = 0$), and the simple Hooke's law is assumed for the concrete in compression and for the mild steel as follows:

Constitutive laws

$$\sigma_d = E_c \varepsilon_d \quad (10)$$

$$f_l = E_s \varepsilon_l \quad (11)$$

$$f_t = E_s \varepsilon_t \quad (12)$$

The simultaneous solution of nine equations, eqns (1)–(3), (6)–(8) and (10)–(12) indicates that the Mohr compatibility truss model satisfies the two-dimensional forces equilibrium, the

Mohr circular compatibility, and Hooke's linear stress–strain relationship. Baumann[8] solved these nine equations to find a formula for the calculation of the angle α. A complete solution algorithm of these nine equations can be found in Hsu's book[13]. This model for linear analysis is applicable only up to the service load stage.

Rotating-angle softened-truss model

The load-deformation history of a membrane element up to failure can be traced by combining the softened constitutive laws with the two-dimensional force equilibrium condition and the Mohr's circular compatibility condition. The result is the rotating-angle softened truss model which is applicable to both the service load stage and the ultimate load stage.

Prior to 1972, the application of the truss model concept to shear and torsion resulted mysteriously in unexplained, exaggerated ultimate strengths. In those days, the failure stress of the concrete struts was assumed to be the uniaxial compression strength of standard concrete cylinders. The first break in this puzzle was Robinson and Demorieux's observation[21] that a reinforced concrete element under shear is actually subjected to a two-dimensional stress condition. The strength in the principal compression direction was found to be softened by the principal tension in the perpendicular direction. This softened stress was referred to as the 'effective stress of concrete'. Researchers were unable to determine this 'effective stress' until Vecchio and Collins[11] constructed a unique 'shear rig', a square steel frame embedded with forty jacks. The jacks were equipped with hinges at both ends to eliminate the edge constraint in biaxial testing of panels. From their shear tests on reinforced concrete panels, Vecchio and Collins[11] proposed the first softened stress–strain curve of concrete under compression. This curve incorporated a softened coefficient which is a function of the principal tensile strain. These researchers then used the softened stress–strain curve of concrete in combination with Mohr's stress and strain circles to predict the load-deformation relationships of reinforced concrete elements.

The softened stress–strain curve of concrete and the stress–strain curve of steel bars recommended below are improved versions developed by Belarbi and Hsu[22,23], Pang and Hsu[24] and Zhang and Hsu[25], Fig. 2. These stress–strain curves are based on the concepts of average (or smeared) stresses and average (or smeared) strains.

Constitutive laws

Concrete in compression – Fig. 2(a)

$$\sigma_d = -\zeta f_c' \left[2\left(\frac{\varepsilon_d}{\zeta \varepsilon_o} \right) - \left(\frac{\varepsilon_d}{\zeta \varepsilon_o} \right)^2 \right]$$

when

$$\frac{\varepsilon_d}{\zeta \varepsilon_o} \leq 1 \tag{13a}$$

$$\sigma_d = -\zeta f_c' \left[1 - \left(\frac{\varepsilon_d/\zeta\varepsilon_o - 1}{2/\zeta - 1} \right)^2 \right]$$

when

$$\frac{\varepsilon_d}{\zeta \varepsilon_o} > 1 \tag{13b}$$

$$\zeta = \frac{5.8}{\sqrt{f_c'(\text{MPa})}} \frac{1}{\sqrt{1 + 400\varepsilon_r}}$$

where

$$\frac{5.8}{\sqrt{f_c'(\text{MPa})}} \leq 0{\cdot}9 \tag{14}$$

Concrete in tension – Fig. 2(b)

$$\sigma_r = E_c \varepsilon_r \text{ when } \varepsilon_r \leq 0{\cdot}00008 \tag{15a}$$

$$\sigma_r = f_{cr} \left(\frac{0{\cdot}00008}{\varepsilon_r} \right)^{0.4} \text{ when } \varepsilon_r > 0{\cdot}00008 \tag{15b}$$

Mild steel – Fig. 2(c)

$$f_s = E_s \varepsilon_s \text{ when } \varepsilon_s \leq \varepsilon_n \tag{16a) or (17a}$$

$$f_s = f_y' = f_y[(0{\cdot}91 - 2B) + (0{\cdot}02 + 0{\cdot}25B)\, \varepsilon_s/\varepsilon_y] \times \left[1 - \frac{2 - \alpha_2/45^\circ}{1000\rho} \right] \text{when } \varepsilon_s > \varepsilon_n$$

(16b) or (17b)

Equations (16a and b) and (17a and b) are two pairs of equations of the same form, one for the longitudinal steel and one for the transverse steel. The factor $[(0{\cdot}91 - 2B) + (0{\cdot}02 + 0{\cdot}25B)$

$(\varepsilon_s/\varepsilon_y)]$ in eqns (16b) and (17b) takes care of the averaging of steel stresses in the post-yield branch. The factor $[1-(2-\alpha_2/45°)/1000\rho]$ takes into account the 'kinking' of reinforcing bars at the cracks.

The 11 governing equations, eqns (1)–(3), (6)–(8), (13a or b), ((14), (15a or b), (16a or b) and (17a or b) encompass 14 unknown variables, including seven stresses (σ_l, σ_t, τ_{lt}, σ_d, σ_r, f_l, f_t) and five strains (ε_l, ε_t, γ_{lt}, ε_d, ε_r), as well as the angle α and the material coefficients ζ. If two unknown variables are given (usually the two applied stresses, σ_l and σ_t) and a third (say, ε_d) is selected, then the remaining 11 unknown variables can be solved by the 11 equations. By selecting a sequence of ε_d values in increments, the shear stress versus shear strain ($\tau_{lt}-\gamma_{lt}$) relationship can be traced. An efficient algorithm to solve this set of 11 equations has been developed[13,26].

Fixed-angle softened-truss model

The three truss models for shear (equilibrium truss model, Mohr compatibility truss model and softened truss model) were developed based on the rotating-angle α. As such, all three models are incapable of predicting the so-called 'contribution of concrete' (V_c). Tests have shown that the shear strength of a membrane element is made of two terms: the 'major term' attributed to steel, and the 'minor term' attributed to concrete. 'Contribution of concrete' (V_c) has baffled many researchers for > 50 years.

The existence of the 'contribution of concrete' (V_c) was explained in Europe by Dei Poli *et al.*[27] and Kupfer and Bulicek[28]. In their truss models the discrete concrete struts were assumed to incline at the fixed angle α_2, Fig. 1(f). Because the fixed angle was not oriented

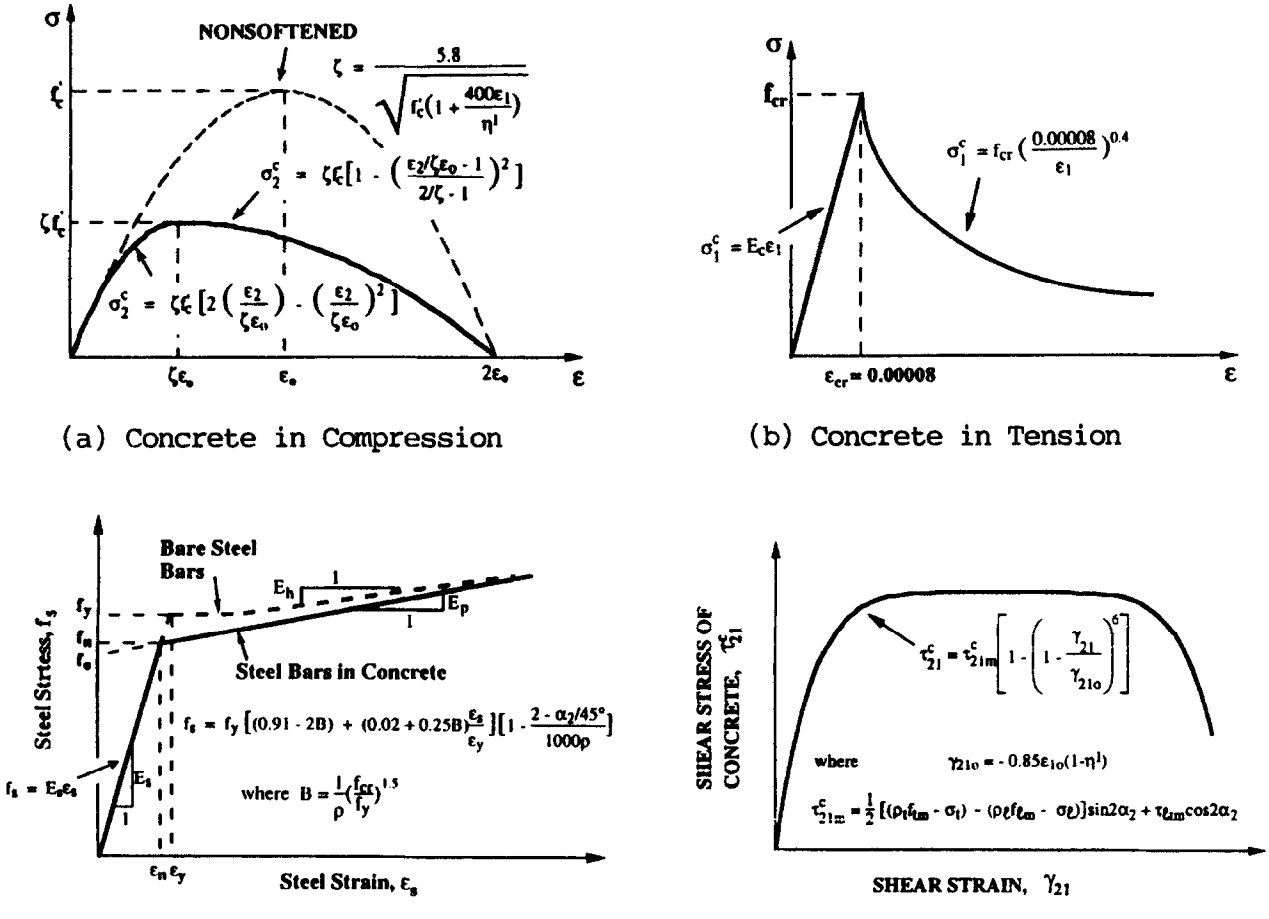

Fig. 2. Constitutive laws of concrete and steel bars in 2–1 coordinate. (a) Concrete in compression (σ_2^c, ε_2 and ε_1 become σ_d, ε_d and ε_r, respectively in d–r coordinates), (b) concrete in tension (σ_1^c and ε_1 become σ_r and ε_r, respectively, under coordinates), (c) steel embedded in concrete and (d) concrete in shear.

in the d-direction of the post-cracking principal stress of concrete, a crack shear stress could exist in the 2-direction, along the concrete struts. These researchers showed that V_c was caused by the crack shear stress of concrete in the 2-direction. In 1996 a fixed-angle softened-truss model was developed on the basis of smeared cracks[14,29]. This model is capable of producing the contribution of concrete (V_c). The equilibrium and compatibility equations for the fixed-angle softened-truss model are derived by transforming the concrete stresses and strains from the 2–1 coordinate to the ℓ–t coordinate.

Equilibrium equations

$$\sigma_\ell = \sigma_2^c \cos^2\alpha_2 + \sigma_1^c \sin^2\alpha_2 + \tau_{21}^c 2\sin\alpha_2\cos\alpha_2 + \rho_\ell f_\ell \quad (18)$$

$$\sigma_t = \sigma_2^c \sin^2\alpha_2 + \sigma_1^c \cos^2\alpha_2 + \tau_{21}^c 2\sin\alpha_2\cos\alpha_2 + \rho_t f_t \quad (19)$$

$$\tau_{\ell t} = (-\sigma_2^c + \sigma_1^c)\sin\alpha_2\cos\alpha_2 + \tau_{21}^c \times (\cos^2\alpha_2 - \sin^2\alpha_2) \quad (20)$$

Compatibility equations

$$\varepsilon_\ell = \varepsilon_2 \cos^2\alpha_2 + \varepsilon_1 \sin^2\alpha_2 + \gamma_{21}\sin\alpha_2\cos\alpha_2 \quad (21)$$

$$\varepsilon_t = \varepsilon_2 \sin^2\alpha_2 + \varepsilon_1 \cos^2\alpha_2 + \gamma_{21}\sin\alpha_2\cos\alpha_2 \quad (22)$$

$$\gamma_{\ell t} = 2(-\varepsilon_2 + \varepsilon_1)\sin\alpha_2\cos\alpha_2 + \gamma_{21} \times (\cos^2\alpha_2 - \sin^2\alpha_2) \quad (23)$$

Constitutive Laws

The four required constitutive laws for rotating-angle theory, represented by the five equations, eqns (13a or b), (14), (15a or b), (16a or b) and (17a or b), are valid for fixed-angle theory, when the stresses and strains in the d–r coordinate, σ_d, σ_r, ε_d and ε_r, are replaced by those in the 2–1 coordinate, σ_2^c, σ_1^c, ε_2 and ε_1, respectively. The only exception is the softening coefficient, ζ, of concrete in the 2–1 direction which is somewhat smaller than that in the d–r direction. Thus, an improvement can be made in eqn (14) to include η' as a parameter[25,29].

In eqns (18)–(23) the crack angle α_2 is no longer an unknown variable because it can be determined directly from the external applied stresses. At the same time, two additional unknowns, τ_{21}^c and γ_{21}, are introduced. These unknowns are related by a constitutive law of shear in cracked concrete, Fig. 2(d):

$$\tau_{21}^c = \tau_{21m}^c\left[1 - \left(1 - \frac{\gamma_{21}}{\gamma_{21o}}\right)^6\right] \quad (24)$$

where τ_{21m}^c is the average shear stress of concrete in the principal 2–1 coordinate at maximum applied stress; and γ_{21o} is the average shear strain corresponding to τ_{21m}^c.

The strain γ_{21o} was found to be

$$\gamma_{21o} = -0{\cdot}85\varepsilon_{1o}(1-\eta') \quad (25)$$

where the strain ε_{1o} is the strain ε_1 at the maximum shear stress $\tau_{\ell tm}$; and $\eta' = (\rho_t f_{ty} - \sigma_t)/(\rho_t f_{ty} - \sigma_t)$ or its reciprocal whichever is less than unity. The average shear stress τ_{21m}^c at maximum applied stress was obtained from the equilibrium of the element:

$$\tau_{21m}^c = \tfrac{1}{2}[(\rho_t f_{ty}' - \sigma_t) - (\rho_\ell f_{\ell y}' - \sigma_\ell)]\sin 2\alpha_2 + \tau_{ltm}\cos 2\alpha_2 \quad (26)$$

where the average yield stresses, $f_{\ell y}'$ or f_{ty}', of embedded steel bars were calculated from eqns (16a or b), (17a or b) and (18).

The 12 governing equations, eqns (13a or b), (14), (15a or b), (16a or b) and (17a or b)–(24), contain 15 unknown variables, including eight stresses (σ_ℓ, σ_t, $\tau_{\ell t}$, σ_2^c, σ_1^c, τ_{21}^c, f_ℓ, f_t), six strains (ε_ℓ, ε_t, $\gamma_{\ell t}$, ε_2, ε_1, γ_{21}), and the material coefficient ζ. If three unknown variables are given (usually σ_ℓ, σ_t and ε_2), then the remaining 12 unknown variables can be solved by the 12 equations. Hsu and Zhang[29] reported an efficient algorithm for solving these 12 equations.

By comparing the three equilibrium equations in the fixed-angle model, eqns (18)–(20), to those in the rotating-angle model, eqns (1)–(3), it becomes clear that eqns (18)–(20) involved additional terms for concrete shear stress τ_{21}^c, which is shown to be responsible for the 'contribution of concrete' (V_c)[14].

APPLICATIONS OF ROTATING-ANGLE SOFTENED-TRUSS MODEL

We will now illustrate the application of the non-linear shear models to actual structures that are subjected predominantly to shear actions. The rotating-angle softened-truss model has been used to analyze and to design low-rise shear walls[30–32], framed shear walls [33] and

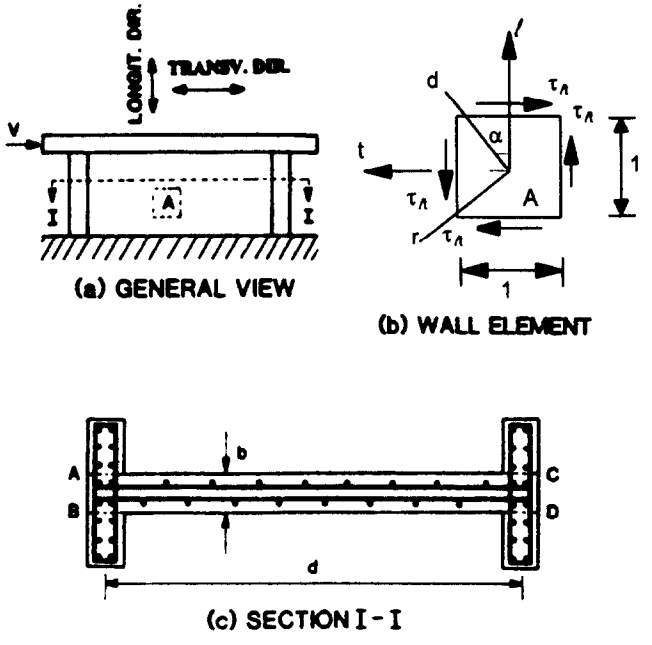

Fig. 3. Low-rise shear walls. (a) General view, (b) wall element and (c) section I–I.

deep beams[34,35]. This models was also applied to study the shear transfer zones, resulting in a more rational shear transfer theory[36,37].

Low-rise shear walls

Low-rise shear walls, Fig. 3, generally refer to shear walls with a height-to-width ratio of less than one, with or without boundary elements. Such walls are used to resist large horizontal forces due to earthquake, while the vertical load is ignored. Wall elements isolated from such shear walls are subjected to pure shear stress τ_{lt}, while the longitudinal and transverse applied stresses are zero (i.e. $\sigma_l = \sigma_t = 0$). Shear deformation, rather than bending deformation, is the primary contributor to the horizontal deflection.

Test specimens simulating such low-rise shear walls are each bounded by a large foundation on the bottom and a large beam at the top. Because the foundation and the beam act like rigid members to constrain the wall in the horizontal direction, the strain in the transverse t-direction (horizontal) can be assumed zero, that is, $\varepsilon_t = 0$. The assumption of $\varepsilon_t = 0$ considerably simplifies the equilibrium and compatibility equations. Substituting $\varepsilon_t = 0$ into eqn (7) and eliminating ε_r from eqn (6) and (7) gives:

$$\varepsilon_l = \varepsilon_d(1 - \tan^2 \alpha) \tag{27}$$

Equation (27) is the only strain compatibility equation that is coupled to the equilibrium and stress–strain equations, because the other compatibility equation, eqn (8), is independent for γ_{lt}.

In addition, because $\varepsilon_t = 0$, f_t must also vanish, and equilibrium eqn (2) becomes uncoupled from the compatibility and stress–strain equations. Since eqn (3) is also an independent equilibrium equation for τ_{lt}, only one equilibrium equation, eqn (1), is coupled to the compatibility and stress–strain equations. Equations (1) and (27) contain five unknowns (ε_d, ε_l, σ_d, f_l and α, with $\sigma_r = 0$). By selecting a value of ε_d, the remaining four variables can be solved by these two equations in conjunction with two stress–strain relationships, one for concrete in compression [eqns (13a or b) and (14) with $\varepsilon_r = \varepsilon_l - \varepsilon_d$] and one for longitudinal steel bars in tension [eqns (16a or b)].

The above simplified solution was used to check 22 low-rise shear walls tested by Barda *et al.*[38], Galletly[39] and Benjamin and Williams[40]. The agreement between the test results and the calculated values was very good[30]. Because of this success, the three failure modes (under-reinforced, balanced and over-reinforced) were identified and a method was proposed for the design of low-rise shear walls[31]. The design method provides two crucial equations:

Balanced shear stress τ_{nb} for design of minimum wall thickness

$$\tau_{nb} = [0{\cdot}365 - 0{\cdot}176\xi + 0{\cdot}028\xi^2] f_c'$$

where
$$\xi = \frac{f_{ly}}{E_s \varepsilon_0} \tag{28}$$

Longitudinal steel ratio ρ_l in the wall:

$$\rho_l = \left[0{\cdot}0013 + 0{\cdot}0984 \frac{\tau_n}{f_c'} + 2{\cdot}209\left(\frac{\tau_n}{f_c'}\right)^2\right] \frac{f_c'}{f_{ly}}$$

where

$$\tau_n = \frac{V_n}{bd} \tag{29}$$

Gupta and Rangan[32] pointed out that the assumption $\varepsilon_t = 0$ provides an upper bound solution for constraint in the transverse direction. If no constraint on the wall is provided by the beam and foundation, the assumption of zero stress in the transverse direction ($\sigma_t = 0$)

would represents the lower bound solution. These authors suggested that within these two boundaries the shear stress–strain relationship of a wall can be determined by the condition: $\cot \alpha = h_w/d_w$, where h_w is the height of the wall, and d_w is the effective horizontal length of the wall. Predicted values agreed fairly well with their test results of eight walls ($h_w/d_w = 1{\cdot}11$) and with other tests in literature.

Frame shear walls

A whole frame shear wall, Fig. 4(a), is made up of a multi-bay and multi-story frame infilled monolithically with wall panels to resist horizontal loads due to earthquake or wind. A unit of frame shear wall, Fig. 4(b), is a rectangular frame (with two columns and two beams) infilled with a wall panel. The columns are subjected to heavy vertical loads to simulate their location at the base story and are subjected to lighter vertical loads if located at the upper stories. An element isolated from the wall panel is subjected to a shear stress $\tau_{\ell t}$ and a vertical (or longitudinal) stress σ_ℓ, Fig. 4(c).

In the case where the frame beams are much larger than the frame columns and the wall panels, as in the test specimens of Tomii and Esaki[41], the assumption of $\varepsilon_t = 0$ and its resulting simplification are valid. When compared to the analysis of low-rise shear walls, the only modification required is to include the vertical stress σ_ℓ in the equilibrium equations. When the beams are large, the magnitude of σ_ℓ can be taken as a uniform stress which is calculated by dividing the total vertical loads by the total cross-sectional areas of the columns and the wall panels. Results of such theoretical analysis compare very well with Tomii and Esaki's experiments.

When frame beams have a comparable cross section as the frame columns, as in the test specimens of Yamada *et al.*[42], the assumption of $\varepsilon_t = 0$ is difficult to justify and the magnitude of vertical stress σ_ℓ in the wall panel becomes difficult to assess. Since flexural hinges were observed to occur at the ends of the beams at ultimate load stage, it was assumed that the uniform vertical stress σ_ℓ on the wall panel had a magnitude that produced the end hinges. Analysis based on these two assumptions was found to be surprisingly accurate in specimens with large vertical loads. Perhaps this is because the non-conservatism of the second assumption for σ_ℓ cancels out the conservatism of the first assumption for ε_t. As expected, this simplified analysis was much too conservative for Yamada *et al.*'s specimens with small vertical loads[33].

Because of the complexity of framed shear walls, an extensive experimental and theoretical research is being carried out at the University of Houston to study their behavior. The frame shear wall unit is 1·067 m (42 in) square on center with 152 mm × 152 mm (6 in × 6 in) cross-sections for both columns and beams. The wall panel is 76 mm (3 in) thick and reinforced with various amount of steel. To date, seven specimens were systematically tested to study the effect of the vertical load and the steel ratio in the wall panels. These specimens will be analyzed by the softened truss model without the two assumptions for ε_t and σ_ℓ, and by a nonlinear finite element program currently being developed.

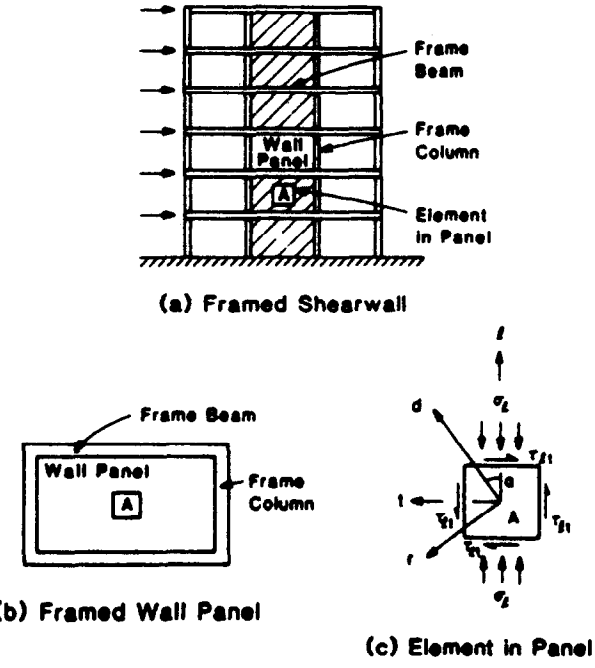

Fig. 4. Framed shear walls.(a) Framed shearwall, (b) framed wall panel and (c) element in panel.

Deep beams

Deep beams, Fig. 5, generally refer to beams with span-to-depth ratio <5 and are loaded on the top face and supported at the bottom face. If a concentrated load is acting on the top surface of a beam, an element isolated from the web between the load and the nearest support reaction (i.e. within the shear span) would be subjected to a shear stress $\tau_{\ell t}$ and a vertical (or

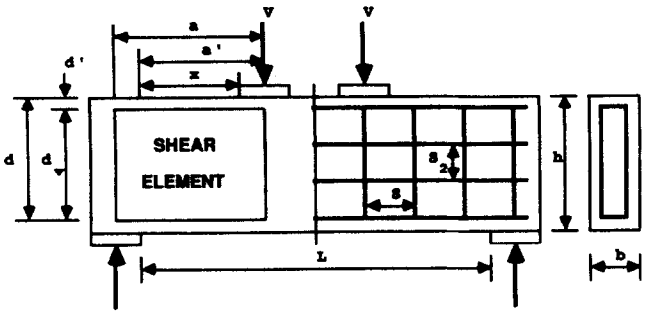

Fig. 5. Deep beams.

transverse) compressive stress σ_t. These two stresses are directly related to the shear force V in the shear span. The shear stress $\tau_{lt} = V/bd_v$, where d_v is the distance between the centroids of the top and bottom stringers. The transverse compressive stress σ_t is not only a function of V, but also a function of the shear-span-ratio a/h, where a is the shear span and h is the total depth of beam. The expression of σ_t as a function of V and a/h is assumed to be:

$$\sigma_t = \frac{V}{bh}\left[\frac{h}{a}\left(\frac{4}{3} - \frac{2}{3}\frac{a}{h}\right)\right]$$

when

$$0{\cdot}5 \leq \frac{a}{h} \leq 2 \tag{30}$$

When $a/h < 0{\cdot}5$, σ_t remains constant at $\sigma_t = 2V/bh$, meaning that the transverse compressive stress is no longer a function of shear-span-ratio a/h. When $a/h \geq 2$, $\sigma_t = 0$, meaning that the effect of the transverse compressive stress vanishes.

Because both τ_{lt} and σ_t are proportional to V, they can be related by an equation

$$\sigma_t = K\tau_{lt} \tag{31}$$

where

$$K = \frac{d_v}{h}\left[\frac{h}{a}\left(\frac{4}{3} - \frac{2}{3}\frac{a}{h}\right)\right]$$

when

$$0{\cdot}5 \leq \frac{a}{h} \leq 2 \tag{32}$$

K, a function of the shear span ratio a/h, becomes $2d_v/h$ when $a/h < 0{\cdot}5$, and becomes zero when $a/h \geq 2$. In view of eqn (31), only one unknown variable σ_l needs to be given (and an addition variable ε_d chosen) before the 11 governing equations [eqns (1)–(3), (6)–(8), (13a or b), (14), (15a or b), (16a or b) and (17a or b)] can be used to solve the 14 unknown variables contained in these equations [seven stresses (σ_l, σ_t, τ_{lt}, σ_d, σ_r, f_l, f_t), five strains (ε_l, ε_t, γ_{lt}, ε_d, ε_r), the angle α and the coefficients ζ]. The algorithm of solution can be further simplified into a computer-friendly iterative solution of five equations using the principle of transformation of stresses and strains[34].

A computer analysis of 64 deep beams with web reinforcement tested by Smith and Vantsiotis[43], Kong *et al.*[44] and De Paiva and Siess[45] shows that the agreement between theory and tests is quite good. The theory correctly predicts that the transverse reinforcement is ineffective in increasing the shear strength in the region of small a/h ratio $< 0{\cdot}5$.

A direct solution of the three equilibrium equations, eqns (1)–(3), leads to the following explicit formula for shear strength of deep beams[35]:

$$\frac{v_u}{f_c'} = \frac{1}{2}\left[K(\omega_l + 0{\cdot}03) + \sqrt{K^2(\omega_l + 0{\cdot}03)^2 + 4(\omega_l + 0{\cdot}03)(\omega_t + 0{\cdot}03)}\right] \leq 0{\cdot}3 \tag{33}$$

where $\omega_l = \rho_l f_{ly}/f_c'$ = reinforcement index in the longitudinal (horizontal) direction, and $\omega_t = \rho_t f_{ty}/f_c'$ = reinforcement index in the transverse (vertical) direction. K is a function of the shear span ratio defined by eqn (32). This rational formula was shown to be superior to all other empirical formulas available in the literature.

Shear transfer strength

The softened truss model was also applied successfully to predict the shear transfer strength of reinforced concrete and to help examine the shear-friction design method adopted in the ACI 318-95 code (Ref. 19 Section 11.7.4). A typical test specimen used in the determination of shear transfer strength, Fig. 6, consists of a panel with a width of h in the longitudinal (horizontal) direction and a transverse (vertical) shear plane of length l in the mid-width of the panel. Two extending arms, one on the top face to the right of the shear plane and the other on

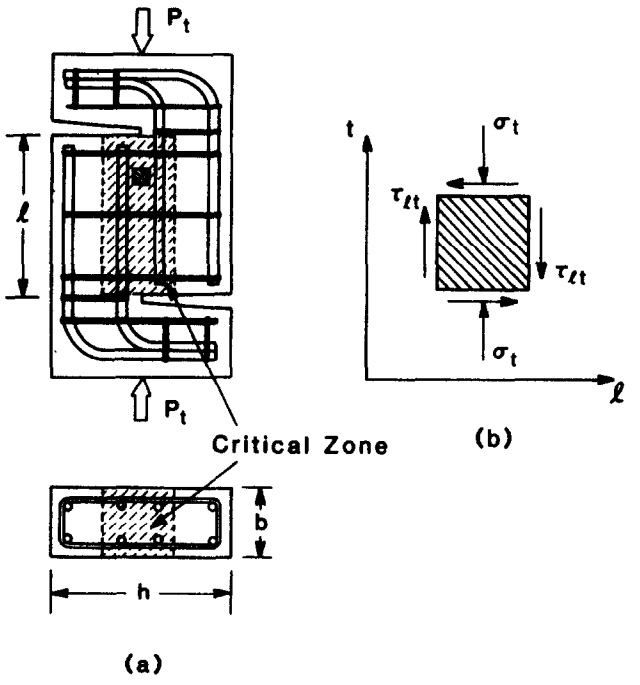

Fig. 6. Shear transfer specimens (push-off type).

the bottom face to the left of the shear plane, are both bent toward the shear plane to form a Z-shape such that a pair of opposing vertical forces P_t can be applied on the arms and along the shear plane. Under a given compression load P_t, diagonal cracks occur along the shear plane in a critical zone of 50–75 mm (2–3 in) wide, which eventually leads to failure. An element isolated from the critical zone is subjected to a shear stress $\tau_{lt} = K_\tau P_t/bl$ and a transverse (vertical) stress $\sigma_t = K_\sigma P_t/bh$, where b is the thickness of the panel; K_τ and K_σ are coefficient describing the non-uniform distribution of stresses.

Because the two applied stresses τ_{lt} and σ_t are both proportional to the external force P_t, eqn (31) applies, except that the proportional constant $K = (l/h)(K_\sigma/K_\tau)$, which is no longer a function of the shear span ratio a/h. In other words, shear friction problem can be viewed as a special case of deep beam when the shear span ratio is reduced to almost zero. In this context, the mathematical solution to the shear transfer problem is identical to that of deep beams described in the previous section. A computer analysis of the specimens tested at the University of Washington[46–48] shows that the best agreement between theory with test results occurs when K_σ/K_τ is taken as unity, resulting in $K = l/h$. Also, the calculated results are shown to be insensitive to changes in K. Furthermore, the effect of increasing the applied tensile stress σ_t on the shear transfer strength is correctly predicted, and the slip measurements across the shear plane indicated good agreement between the theoretical and experimental shear strains at peak stress. All these observations lead to the conclusion that the softened truss model can correctly predict the shear transfer strength and the slip deformation of shear plane.

The softened truss model has helped to identify the governing parameters that effect the shear transfer strength. In the 1980s, Delft University of Technology, Netherlands, carried out extensive tests of shear transfer specimens[49]. This study covered a wide range of concrete strengths ($17{\cdot}5\ \text{MPa} < f_c' < 65\ \text{MPa}$) and 'smeared steel stresses' ($0{\cdot}35\ \text{MPa} < \rho_t f_{ty} < 15\ \text{MPa}$). Based on statistical analyses of 88 test specimens, these researchers derived a best-fit formula as follows:

$$v_u = 0{\cdot}822(f_{cc}')^{0{\cdot}406}(\rho_t f_{ty})^c$$

where

$$c = 0{\cdot}159(f_{cc}')^{0{\cdot}303} \tag{34}$$

[In eqn (34) f_{cc}' is the concrete compressive strength of 150 mm cubes and is taken as $f_c'/0{\cdot}85$. The values of f_{cc}', $\rho_t f_{ty}$ and v_u must be in MPa]. However, the softened truss model, shown by eqn (33), predicts that the normalized shear strength, v_u/f_c', should be a function of the non-dimensionalized reinforcement index $\omega_t = \rho_t f_{ty}/f_c'$, while neglecting ω_t and taking K as a constant. Using ω_t as the sole parameter, Mau and Hsu [36] found a very simple formula that fits the 88 test results with virtually the same degree of accuracy as that of eqn (34):

$$\frac{v_u}{f_c'} = 0{\cdot}66\sqrt{\omega_t} \leq 0.3 \tag{35}$$

Equation (35) has the advantage of being simple, as well as being dimensionally correct. It has been accepted by Walraven *et al.*[50] as the more desirable formula than their own, and is currently being promoted for use in Europe.

FINITE ELEMENT APPLICATIONS

The power of the modern computer and the development of the finite element method have made it possible to perform rational analyses on the behavior of large and complex reinforced

concrete structures, for example, shear walls, box bridges, nuclear containment vessels, concrete offshore structures, etc. Because these structures can be visualized as assemblies of membrane elements, their behaviors can be predicted if the behaviors of the membrane elements are known.

When the finite element method is applied to reinforced concrete structures, the mechanical properties of concrete and steel bars are represented by material stiffness matrices. In establishing the concrete stiffness matrix, two models are used: the *rotating-crack model*, in which the cracks are assumed to orient in the principal directions of the cracked concrete (d–r coordinate); and the *fixed-crack model*, in which the cracks are fixed at the orientation determined by the principal directions of the applied stresses (2–1 coordinate).

The stress–strain relationships of concrete based on the rotating-crack model (principal d–r coordinates) are expressed as follows:

$$\begin{Bmatrix} \sigma_d \\ \sigma_r \\ \tau_{dr} \end{Bmatrix} = \begin{bmatrix} \bar{E}_d & 0 & 0 \\ 0 & \bar{E}_r & 0 \\ 0 & 0 & \bar{G}_{dr} \end{bmatrix} \begin{Bmatrix} \varepsilon_d \\ \varepsilon_r \\ \gamma_{dr} \end{Bmatrix} \tag{36}$$

The 3×3 matrix in eqn (36) represents the cracked concrete stiffness matrix. Here, the diagonal elements $\bar{E}_d$ and $\bar{E}_r$ are the secant moduli of concrete in the d- and r-directions, and $\bar{G}_{dr}$ is the secant shear modulus of concrete in the principal d–r direction. The moduli $\bar{E}_d$ and $\bar{E}_r$ are determined from the constitutive laws of concrete established experimentally in the rotating-angle softened-truss model. However, $\bar{G}_{dr}$ cannot be determined from tests because shear stresses and shear strains cannot exist in the principal d–r direction. In practice, therefore, $\bar{G}_{dr}$ is arbitrarily taken as a fraction of the uncracked concrete shear modulus to fit the overall test results. This practice is theoretically unsound.

At present, research is being carried out at the University of Houston to establish a more general stress–strain relationship of concrete that is based on the fixed-crack model (principal 2–1 coordinate) and includes the Poisson ratios:

$$\begin{Bmatrix} \sigma_2^c \\ \sigma_1^c \\ \tau_{21}^c \end{Bmatrix} = \begin{bmatrix} \bar{E}_2 & \nu_{12}\bar{E}_2 & 0 \\ \nu_{21}\bar{E}_1 & \bar{E}_1 & 0 \\ 0 & 0 & \bar{G}_{21} \end{bmatrix} \begin{Bmatrix} \varepsilon_2 \\ \varepsilon_1 \\ \gamma_{21} \end{Bmatrix} \tag{37}$$

In the concrete stiffness matrix, the diagonal elements $\bar{E}_2$ and $\bar{E}_1$ are the secant moduli of concrete in the 2- and 1-directions, respectively, and $\bar{G}_{21}$ is the secant shear modulus of concrete in the 2-1 coordinate. The symbols ν_{12} and ν_{21} in the non-diagonal elements are the Poisson ratios. The three moduli $\bar{E}_2$, $\bar{E}_1$ and $\bar{G}_{21}$ and the two Poisson ratios ν_{12} and ν_{21} will be determined from new strain-controlled tests of reinforced concrete panels.

The assumption that Poisson ratios are zero underpins the basic concept of the truss models. When Poisson ratios are included in the analysis, the term 'truss model' is no longer valid.

CONCLUDING REMARKS

In just 130 years of existence, reinforced concrete has established itself as the predominant construction material worldwide. It is the primary material that builds the foundation for industrialization in developing countries, and is the material of choice for renovating infrastructures in more developed countries. Reinforced concrete is affordable, easy to use, and is the only material that can be mass produced for the benefit of all humankind across economic strata. Furthermore, reinforced concrete as an industry is non-intrusive to the environment and can sustain growth without exhausting its raw materials. The use of reinforced concrete is expected to continue into the future, building clean environments and raising living standards all over the world.

Increasing utilization of reinforced concrete demands the development of rational theories for reinforced concrete behavior. Each advancement in reinforced concrete theory infers a significant economic and broad-ranged impact. A rational theory for bending and axial load (Bernoulli compatibility truss model) was established in the 1960s. This theory satisfied Navier's three principles of mechanics of materials, namely, the parallel stress equilibrium, Bernoulli's linear compatibility and the uniaxial constitutive laws of concrete. From the 1960s to the present year, we witness the development of a consistent set of four rational models for shear and torsion. The two nonlinear models for shear and torsion (softened truss models) also satisfies Navier's three principles of mechanics of materials: two-dimensional stress equilibrium, Mohr's circular compatibility and the softened biaxial constitutive laws of concrete. The integration of

all the rational theories for the four actions (bending, axial load, shear and torsion) gave rise to the unified theory of reinforced concrete.[51]

This paper chronicles the unified approach for shear analysis and design developed over the past three decades. It describes the strut-and-tie model, the equilibrium (plasticity) truss model, the Mohr compatibility truss model, the rotating-angle softened-truss model, as well as the new fixed-angle softened-truss model. Then it addresses the application of the rotating-angle softened-truss model to low-rise shear walls, framed shear walls, deep beams and shear transfer strength. It concludes with a discussion of the increasing application of computer-aided finite element method in reinforced concrete structures, and the need to establish a concrete stiffness matrix which is based on the fixed crack model and includes the Poisson's ratios.

ACKNOWLEDGEMENTS

Research required to develop the unified approach to shear analysis and design was sponsored by a series of grants from National Science Foundation.

REFERENCES

1. Navier, C. L., *Resume des lecons donnees a l'ecole des ponts et chaussees sur l'application de la mecanique a l'establissement des constructions et des machines*. Firmin Didet, Paris, 1826.
2. Hognestad, E., Hanson, N. W. & McHenry, D., Concrete Stress Distribution in Ultimate Strength Design. *Journal of the American Concrete Institute*, **52**(4), Dec. (1955) 455–479.
3. Whitney, C. S., Plastic theory of reinforced concrete design. *Proceedings, ASCE Transaction V.*, **107** (1942) 251–282.
4. Ritter, W., *Die Bauweise Hennebique*. Schweizerishe Bauzeitung, Zurich, Switzerland, 1899.
5. Mörsch, E., Der Eisenbetonbau, seine Anwendung und Theorie, 1st ed. Wayss and Freytag, A. G., Im Selbstverlag der Firma, Neustadt a. d. Haardt, Germany, 1902.
6. Nielsen, M. P., Om Forskydningsarmering i Jernbetonbjaelker (On Shear Reinforcement in Reinforced Concrete Beams). Bygningsstatiske Meddelelser, Copenhagan, Denmark, vol. 38, No. 2, pp. 33–58, 1967.
7. Lampert, P. & Thurlimann, B., Torsion Tests of Reinforced Concrete Beams (Torsionsversuche an Stahlbetonbalken), *Bericht No. 6506-2*, Institute fur Baustatik, ETH, Zurich, Switzerland, 1968.
8. Baumann, T., Zur Frage der Netzbewehrung von Flachentragwerken. *Der Bauingenieur*, **47**(6) (1972) 367–377.
9. Collins, M. P., Torque-twist characteristics of reinforced concrete beams. In: *Inelasticity and Non-linearity in Structural Concrete*, Study No. 8, University of Waterloo Press, pp. 211–231, 1973.
10. Collins, M. P. & Mitchell, D., Shear and torsion design of prestressed and non-prestressed concrete beams. *Journal of the Prestressed Concrete Institute*, **25**(5), Sept.-Oct. (1980) 32–100.
11. Vecchio, F. & Collins, M. P., Stress–strain characteristics of reinforced concrete in pure shear. *Final Report*, IABSE Colloquium on Advanced Mechanics of Reinforced Concrete, Delft, Netherland, pp. 211–225, 1981.
12. Hsu, T. T. C., Softening truss model theory for shear and torsion. *Structural Journal of the American Concrete Institute*, **85**(6), Nov.-Dec. (1988) 624–635.
13. Hsu, T. T. C. *Unified Theory of Reinforced Concrete*. CRC Press, Boca Raton, FL, 1993.
14. Pang, X. B. & Hsu, T. T. C., Fixed-angle softened-truss model for reinforced concrete. *Structural Journal of the American Concrete Institute*, **93**(2), Mar.-Apr. (1996) 197–207.
15. Schlaich, J., Schafer, K. & Jennewein, M., Toward a consistant design of structural concrete. *Journal, Prestressed Concrete Institute*, **32**(3), May-June (1987) 74–150.
16. Elfgren, L., Reinforced concrete beams loaded in combined torsion, bending and shear. Publication 71:3, Division of Concrete Structures, Chalmers University of Technology, Goteborg, Sweden, 1972.
17. CEB (Comite Euro-International du Beton), *Model Code for Concrete Structures*. CEB-FIP International Recommendation, 3rd Edn, 1978.
18. CEB (Comite Euro-International du Beton), *CEB-FIP Model Code 1990*. Thomas Telford Services Ltd, London, 1990.
19. ACI-318, *Building Code Requirements for Structural Concrete (ACI 318-95) and Commentary (ACI 318R-95)*, American Concrete Institute, Farmington Hill, MI, 1995.
20. Hsu, T. T. C., ACI shear and torsion provisions for prestressed hollow girders. *Structural Journal of the American Concrete Institute*, **94**(6), Nov.-Dec. (1997) 787–799.
21. Robinson, J. R. & Demorieux, J. M., Essais de Traction-compression sur Modeles d'ame de Poutre en Beton Arme. In: *IRABA Report*, Institut de Recherches Appliquees du Beton de L'ame, Paris, France, Part 1, June 1968, and Part 2, Resistance Ultimate du Beton de L'ame de Poutres en Double Te en Beton Arme, May, 1972.
22. Belarbi, A. & Hsu, T. T. C., Constitutive laws of concrete in tension and reinforcing bars stiffened by concrete. *Structural Journal of the American Concrete Institute*, **91**(4), July-August (1994) 465–474.
23. Belarbi, A. & Hsu, T. T. C., Constitutive laws of softened concrete in biaxial tension–compression. *Structural Journal of the American Concrete Institute*, **92**(5), Sept.-Oct. (1995) 562–573.
24. Pang, X. B. & Hsu, T. T. C., Behavior of reinforced concrete membrane elements in shear. *Structural Journal of the American Concrete Institute*, **92**(6), Nov.-Dec. (1995) 665–679.
25. Zhang, L. X. & Hsu, T. T. C., Behavior and analysis of 100 MPa concrete membrane elements. *Journal of Structural Engineering, ASCE*, **124**(1), Jan. (1998) 24–34.
26. Hsu, T. T. C., Nonlinear analysis of concrete mem-

brane elements. *Structural Journal of the American Concrete Institute*, **88**(5), Sept.-Oct. (1991) 552–561.
27. Dei Poli, S., Gambarova, P. G. & Karakoc, C., Aggregate interlock role in R. C. thin webbed beams in shear. *Journal of Structural Engineering, ASCE*, **113**(1), January (1987) 1–19.
28. Kupfer, H. & Bulicek, H., A consistent model for the design of shear reinforcement in slender beams with I- or box-shaped cross section. In: *Concrete Shear in Earthquake*, Edited by Hsu & Mau, Proceedings of the International Workshop on Concrete Shear in Earthquake, 14–16 January, 1991, Houston. Elsevier Science, London, January, pp. 256–265, 1992.
29. Hsu, T. T. C. & Zhang, L. X., Nonlinear analysis of membrane elements by fixed-angle softened-truss model. *Structural Journal of the American Concrete Institute*, **94**(5), Sept.-Oct. (1997) 483–492.
30. Hsu, T. T. C. & Mo, Y. L., Softening of concrete in low-rise shear walls. *Journal of the American Concrete Institute*, **82**(6), Nov.-Dec. (1985) 883–889.
31. Mau, S. T. & Hsu, T. T. C., Shear design and analysis of low-rise structural walls. *Journal of the American Concrete Institute*, **83**(2), Mar.-Apr. (1986) 306–315.
32. Gupta, A. & Rangan, B. V., *Studies on Reinforced Concrete Structural Walls*, Research Report No. 2/96, School of Civil Engineering, Curtin University of Technology, Perth, Western Australia, Australia, May, 1996.
33. Mau, S. T. & Hsu, T. T. C., Shear behavior of reinforced concrete framed wall panels with vertical loads. *Structural Journal of the American Concrete Institute*, **84**(3), May-June (1987) 228–234.
34. Mau, S. T. & Hsu, T. T. C., Shear strength prediction for deep beams with web reinforcement. *Structural Journal of the American Concrete Institute*, **84** 6, Nov.-Dec. (1987) 513–523.
35. Mau, S. T. & Hsu, T. T. C., Formula for the shear design of deep beams. *Structural Journal of the American Concrete Institute*, **86**(5), Sept.-Oct. (1989) 516–523.
36. Mau, S. T. & Hsu, T. T. C., Discussion of a paper: "Influence of Concrete Strength and Load History on the Shear Friction Capacity of Concrete Members" by Walraven, Frenay and Pruijssers. *Journal of the Prestressed Concrete Institute*, **33**(1), Jan.-Feb. (1988) 166–168.
37. Hsu, T. T. C., Mau, S. T. & Chen, B., A theory on shear transfer strength of reinforced concrete. *Structural Journal of the American Concrete Institute*, **84**(2), Mar.-Apr. (1987) 149–160.
38. Barda, F., Hanson, J. M. & Corley, W. G., Shear strength of low-rise walls with boundary elements. Research and Development Bulletin No. RD043D, Portland Cement Association, Skokie, IL, 1976.
39. Galletly, G. D., Behavior of reinforced concrete shear walls under static load. In: *Report of Department of Civil and Sanitary Engineering*, Massachusetts Institute of Technology, Cambridge, MA, August, 1952.
40. Benjamin, J. R. & Williams, H. A., The behavior of one story reinforced concrete shear walls. *Proceedings ASCE*, **83**(ST3), May (1957) 1254
41. Tomii, M. & Esaki, F., Design method of reinforced concrete framed shear walls to sustain vertical loads after shear failure. In: *Proceedings, 8th World Conference on Earthquake Engineering*, San Francisco, Vol. 5, pp. 581–588, 1984.
42. Yamada, M., Kawamura, H. & Katagihara, K., Reinforced concrete shear walls without openings; test and analysis. In: *Shear in Reinforced Concrete*, SP-42, American Concrete Institute, Detroit, pp. 539–558, 1974.
43. Smith, K. N. & Vansiotis, A. S., Shear strength of deep beams. *Journal of the American Concrete Institute*, **79**(3), May-June (1982) 201–213.
44. Kong, F. K., Robin, P. J. & Cole, D. F., Web reinforcement effect on deep beams. *Journal of the American Concrete Institute*, **67**(12), Dec. (1970) 1010–1017.
45. De Paiva, H. A. R. & Siess, C. P., Strength and behavior of deep beams in shear. *Proceedings, ASCE*, **91**(ST5), Oct. (1965) 19–41.
46. Hofbeck, J. A., Ibrahim, I. O. & Mattock, A. H., Shear transfer in reinforced concrete. *Journal of the American Concrete Institute*, **66**(2), Feb. (1969) 119–128.
47. Mattock, A. H., Effect of aggregate type on single direction shear transfer strength in monolithic concrete. In: Report No. SM74-2, Department of Civil Engineering, University of Washington, Seattle, WA, August, 1974.
48. Mattock, A. H., Li, W. K. & Wang, T. C., Shear transfer in lightweight reinforced concrete. *Journal of the Prestressed Concrete Institute*, **21**(1), Jan-Feb. (1976) 20–39.
49. Walraven, J., Frenay, J. & Pruijssers, A., Influence of concrete strength and load history on the shear friction capacity of concrete members. *Journal of the Prestressed Concrete Institute*, **32**(1), Jan.-Feb. (1987) 66–84.
50. Walraven, J., Frenay, J. & Pruijssers, A., Closure on their paper 'Influence of concrete strength and load history on the shear friction capacity of concrete members'. *Journal of the Prestressed Concrete Institute*, **33**(1), Jan.–Feb. (1988) 169–170.
51. Hsu, T. T. C., Toward a unified nomenclature for reinforced concrete theory. *Journal of Structural Engineering, ASCE*, **122**(3), March (1996) 275–283.